Particle Physics 2: Quantum Chromodynamics

Prof. Dr. Juan Rojo
VU Amsterdam and Nikhef Theory Group
http://www.juanrojo.com/
j.rojo@vu.nl

5 QCD in proton-proton collisions

In the previous lectures we have studied the implications of of perturbative QCD corrections for two important classes of processes in particle physics:

- First, **jet production in electron-positron annihilation**, a process without hadrons in the initial state. There we found that soft and collinear singularities cancel in inclusive enough observables such as a IRC-safe jet cross-section.
- Second, **lepton-proton deep-inelastic scattering**, a process with one hadron in the initial state. There, initial-state collinear singularities do not cancel even for inclusive observables, but they can be absorbed into a redefinition of the PDFs, inducing a scale dependence determined by the DGLAP evolution equations.

In this lecture we study QCD in the context of proton-proton collisions, such as those taking place at the Large Hadron Collider (LHC) at CERN in Geneva. This is a process which contains two hadrons in the initial state, and in which again novel QCD phenomena arise which were absent from the processes studied so far. We will also discuss a number of techniques which enable the simulation and interpretation of measurements carried out in proton-proton collisions, which represent a key component of the modern toolbox for particle physics.

Learning Goals of the Lecture

- Identify the most hard processes in proton-proton collisions and the mean features of the associated cross-sections.
- Determine the underlying mechanisms describing the numerical simulation of high-energy proton-proton collisions.
- Apply jet production algorithms to proton-proton collisions and identify the main concepts in jet substructure analyses.

5.1 Kinematics of proton-proton collisions

To begin with, we will discuss which kinematic variables are suitable to describe the outcome of hadron-hadron collisions. A key difference as compared to e^+e^- annihilation is the following:

The initial state of proton-proton collisions

In hadronic collisions, we know the total momentum of the colliding **protons**, but not that of the colliding **partons**. As we have seen in the previous lecture, the distribution of momentum carried by the quarks and gluons within the proton is given by the parton distribution functions. In other words, even if the total energy of the colliding protons is fixed, the energy of the colliding partons will be **different in each event**.

For instance, assume the collision of two protons with energy $E_1 = E_2 = \sqrt{s}/2$, with $\sqrt{s}$ being the total center of mass energy. The energy available for the partonic reaction will $\sqrt{\hat{s}} = \sqrt{x_1 x_2 \sqrt{s}}$, with x_1 being the momentum fraction associated to the colliding parton in the first proton and conversely for x_2, where recall that we indicate with a hat the partonic variables. To show this, we can write hadronic and partonic momenta as follows:

$$p_1 = (E_1, 0, 0, E_1) \tag{5.1}$$
$$p_2 = (E_2, 0, 0, -E_2) \tag{5.2}$$
$$\hat{p}_1 = (x_1 E_1, 0, 0, x_1 E_1) \tag{5.3}$$
$$\hat{p}_2 = (x_2 E_2, 0, 0, -x_2 E_2) \tag{5.4}$$

where we neglect finite masses, and therefore we have that:

$$(p_1 + p_2)^2 = (E_1 + E_2)^2 - (E_1 - E_2)^2 = 4E_1^2 \,, \tag{5.5}$$

since $E_1 = E_2$, and hence $s = 4E_1^2$ and $E_1 = \sqrt{s}/2$ as expected. In the case of the partonic momenta instead, one has that

$$\hat{s} = (\hat{p}_1 + \hat{p}_2)^2 = (x_1 E_1 + x_2 E_2)^2 - (x_1 E_1 - x_2 E_2)^2 = 4 x_1 x_2 E_1^2 = x_1 x_2 s \,, \tag{5.6}$$

so indeed we see that, due to the fact that protons are not elementary particles but instead they are composed by quarks and gluons, the total energy of the collision is reduced by a factor $\sqrt{x_1 x_2}$ in terms of the momentum fraction carried out by the colliding partons in the proton. As mentioned above, the latter will be different event by event.

Discussion #5.1

The LHC has a total hadronic center of mass energy of $\sqrt{s} = 13.6$ TeV. Does it mean that it can produce particles in an $s-$**channel reaction** of the form $pp \to X$ up to masses of $m_X = 13.6$ TeV? Or do you think that instead only lower masses will be accessible and why? And is there a **lower limit** on how small the mass m_X of the produced particle can be?

Since in general the partonic momentum fractions x_1 and x_2 carried by the quarks will be different, $x_1 \neq x_2$, even if the hadronic collision is symmetry is clear that the **partonic collision will be asymmetric**. Indeed, from the derivation above we see that

$$p_{1+2} = p_1 + p_2 = (2E, 0, 0, 0) \,, \tag{5.7}$$

$$\hat{p}_{1+2} = \hat{p}_1 + \hat{p}_2 = ((x_1 + x_2)E, 0, 0, (x_1 - x_2)E) \,, \tag{5.8}$$

and hence indeed the resulting final state of the partonic collision with the boosted in the direction of either the first incoming proton (for $x_1 > x_2$) or the second incoming proton (for $x_2 > x_1$). This also implies that

in general, the hadronic center of mass frame will be different to the partonic center of mass frame, and these two frames will only coincide when the colliding partons carry the same momentum fraction, $x_1 = x_2$. Therefore, in hadronic collisions, the most suitable event description is provided by quantities that are either invariant or that transform in a simple way **under longitudinal boosts**. The reason is that, event by event, the initial state longitudinal momentum of the partonic collision is unknown, since it is determined stochastically in terms of the PDFs $f_i(x, Q^2)$.

Proton-ion collisions at the LHC

In addition to proton-proton collisions, the LHC can also collide heavy ions (such as lead nuclei) among them as well as proton-ion collisions. The latter are **asymmetric** already at the hadronic level, since the energy that heavy ions can achieve within the LHC accelerator chair is smaller than the energy that protons can achieve. Since in this case boost is known and constant for all collisions, it is possible too to change reference frame from the lab frame to the center of mass frame, where the two colliding species have the same energy.

For this reason, experimental measurements in proton-proton collisions are usually expressed in terms of the following parameterization for four-momenta. In the following we will adopt:

$$p^\mu = (E, p_x, p_y, p_z) = \left(\sqrt{\vec{p}^2 + m^2}, |\vec{p}| \sin\theta \, \cos\phi, |\vec{p}| \sin\theta \, \sin\phi, |\vec{p}| \cos\theta\right) \tag{5.9}$$

where θ is the polar angle with respect to the hadron beam and ϕ is the azimuthal angle with respect also to the hadron beam axis, as shown in Fig. 5.1, and m is the particle mass. You can verify that this parametrisation of p^μ satisfies the on-shell condition, given that

$$p^2 = (\vec{p}^2 + m^2) - \vec{p}^2 = m^2 \, . \tag{5.10}$$

It is customary to express the four-momentum p^μ in terms of the rapidity y and the transverse mass m_T, defined respectively as

$$y \equiv \frac{1}{2} \ln \frac{E + p_z}{E - p_z} \, , \qquad m_T \equiv \sqrt{p_T^2 + m^2} \, , \tag{5.11}$$

such that the parametrisation Eq. (5.9) can be written as follows

$$p^\mu = (E, p_x, p_y, p_z) = (m_T \cosh \, y, |p_T| \cos\phi, |p_T| \sin\phi, m_T \sinh \, y) \, , \tag{5.12}$$

where

$$\vec{p_T} = (p_x, p_y) \, , \quad p_T = |\vec{p_T}| = |\vec{p}| \sin\theta \, , \tag{5.13}$$

is the **transverse momentum** of the particle, that is, the component of the tri-momentum perpendicular to the proton-proton collision axis.

As mentioned above, for hadronic collisions it is advantageous to express observables in terms of quantities which are either invariant of that transform easily under longitudinal boosts. In Eq. (5.12), the transverse mass and the p_T are by construction invariant under longitudinal boosts (that is, a Lorentz transformation aligned with the z direction), while the rapidity transforms additively,

$$y \to y' = y + y_{\rm boost} \, , \qquad y_{\rm boost} = \tanh^{-1}(v/c) = \frac{1}{2} \ln \frac{x_1}{x_2} \, , \tag{5.14}$$

with v being the relative velocity of the new reference frame. In particular, this means that going from the hadronic to the partonic reference frame will only shift the rapidity y distributions by a **constant factor**.

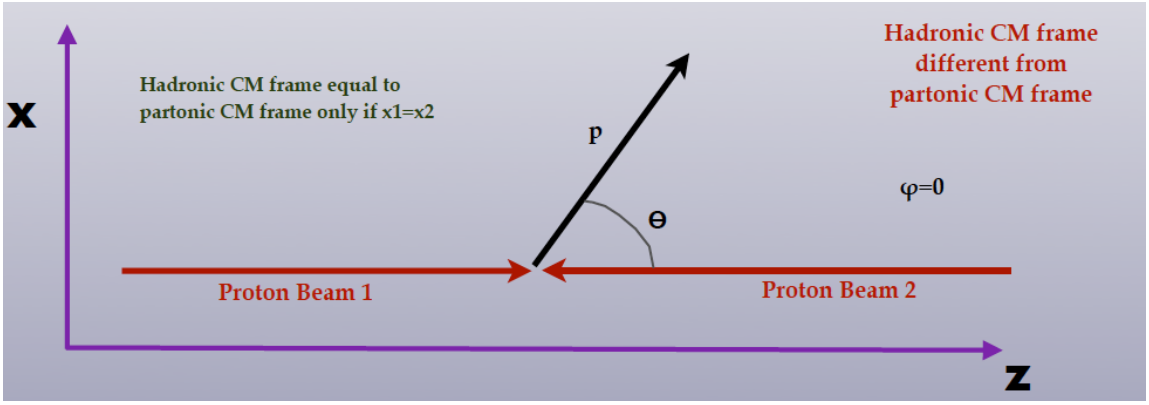

Figure 5.1. Kinematics of an hadron-hadron collision for an azimuthal angle of $\phi = 0$. In general, the hadronic center of mass frame will be different to the partonic center of mass frame.

Discussion #5.2

Will the difference between the rapidities of two particles $\Delta y \equiv y_1 - y_2$ be the same in the hadronic and partonic reference frames or it will be different? If I want to carry out a measurement which provides information on the momentum fractions x_1 and x_2 carried by the colliding protons, what os best, a measurement in terms of $y_1 + y_2$ or a measurement in terms of Δy?

To derive Eq. (5.12) from Eq. (5.9), note that

$$\cosh y = \frac{1}{2}\left(\left(\frac{E+p_z}{E-p_z}\right)^{1/2} + \left(\frac{E-p_z}{E+p_z}\right)^{1/2}\right) = \frac{E}{\sqrt{m^2+p_T^2}} = \frac{E}{m_T}\,, \tag{5.15}$$

and likewise for the other component of the four-momentum, where we have used that

$$\cosh y = \frac{1}{2}\left(e^y + e^{-y}\right) \tag{5.16}$$

together with Eq. (5.11) and the fact that $E^2 = m^2 + p_z^2 + p_T^2$.

As you have learned in your special relativity course, it is easy to show that the rapidity y transforms additively under longitudinal boosts. To prove this, recall that under a longitudinal boost (that is, a boost in the z direction, the beam direction), a four-momentum transforms as

$$p^\mu \quad \rightarrow \quad p'^\mu = \gamma\left(E - \beta\, p_z,\, p_x\,, p_y\,, -\beta\, E + p_z\right)\,, \tag{5.17}$$

in terms of the usual Lorentz boost parameters

$$\beta = \frac{v}{c}\,, \qquad \gamma = \frac{1}{\sqrt{1-v^2/c^2}}\,, \tag{5.18}$$

so one finds that the rapidity transforms as

$$y \quad \rightarrow \quad y' = y + \frac{1}{2}\log\frac{1-\beta}{1+\beta}\,, \tag{5.19}$$

given that

$$E \rightarrow E' = E - \beta p_z\,, \quad p_z \rightarrow p_z' = -\beta E + p_z\,, \tag{5.20}$$

which has the important consequence that the difference between rapidities is boost invariant:

$$\Delta y' \equiv y'_1 - y'_2 = \Delta y \equiv y_1 - y_2 \,, \tag{5.21}$$

and thus should be less sensitive to the details of the PDFs than other kinematic variables. This derivation motivates the use of transverse variables and of the rapidity y to describe the kinematics of hadronic collisions.

In the limit of massless particles (defined as the limit in which $m \ll p_T, E$), the rapidity simplies to a quantity known as *pseudo-rapidity*,

$$y \simeq \eta \equiv -\log \tan \frac{\theta}{2} \,, \tag{5.22}$$

which is often used in experimental analyses since it can be directly related to the geometrical acceptance of the detector (since it is expressed in terms of the polar angle of the particle). To verify this property, note that when $m \ll p_T$, then $m_T \simeq p_T$, and therefore the four momentum of a massless particle becomes

$$p \simeq p_T \left(\cosh y, \cos\phi, \sin\phi, \sinh y\right) \,, \tag{5.23}$$

and therefore we can write the rapidity as

$$y = \frac{1}{2} \ln \frac{E + p_z}{E - p_z} \simeq \frac{1}{2} \ln \frac{1 + \cos\theta}{1 - \cos\theta} = -\ln \tan \frac{\theta}{2} = \eta \tag{5.24}$$

where we have used $p_z \simeq E \cos\theta$ for massless particles.

Central vs forward production in proton+proton collisions

Achieving the maximum coverage in pseudo-rapidity is an important feature of a detector for hadron colliders, since this way one can access processes in the forward region. In Fig. 5.2 we show the approximate coverage in transverse momentum p_T and pseudo-rapidity η of current (and proposed) LHC detectors. The two main purpose detectors, ATLAS and CMS, can cover up to $\eta \sim 2.5$, extended to $\eta \sim 4$ with the forward calorimeters, while LHCb is a forward experiment with acceptance $2.0 \leq \eta \leq 4.5$.

Discussion #5.3

Since a few years, the ForwArd SEarch ExpeRiment (FASER) enables the detection of particles produced at **very forward rapidities**, $\eta \gtrsim 8.5$. Discuss whether this experiment could be placed near the ATLAS detector or instead it needs to be placed far away. FASER makes possible measurements of interaction cross-sections relevant for **cosmic ray physics**: explain this connection and determine the typical energies of the cosmic rays that can be probed at the FASER kinematics.

Another useful relation is provided by the phase space in these new coordinates, which reads

$$\frac{d^3p}{2E(2\pi)^2} = \frac{1}{2(2\pi)^3} d^2p_T \, dy \,, \tag{5.25}$$

as can be checked from the Jacobian of the change of variables

$$dp_x \, dp_y \, dp_z = \left| \left(\frac{\partial(p_x, p_y, p_z)}{\partial(p_T, y, \phi)} \right) \right| dp_T \, dy \, d\phi \tag{5.26}$$

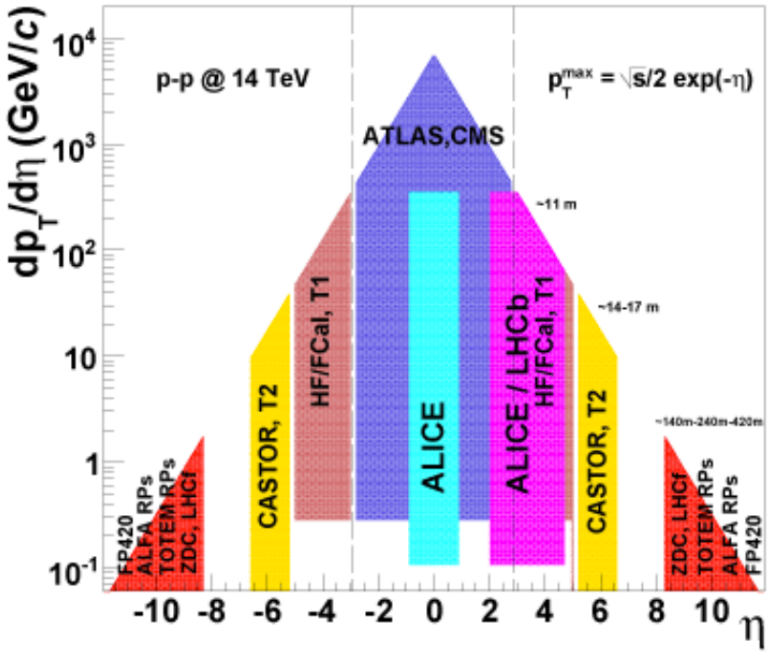

Figure 5.2. Approximate coverage in transverse momentum p_T and pseudo-rapidity η of current and future LHC detectors. For a given $\sqrt{s}$ and pseudo-rapidity η, the kinematically maximum available p_T is $p_T^{\rm max} \simeq \sqrt{s}e^{-y}/2$.

$$d^3p = \left| \begin{pmatrix} p_T \cosh y & 0 & \sinh y \\ 0 & -p_T \sin\phi & \cos\phi \\ 0 & p_T \cos\phi & \sin\phi \end{pmatrix} \right| dp_T\, dy\, d\phi\,, \tag{5.27}$$

which is the expression that is used in calculations of hadronic processes. This is another useful property of the parametrization Eq. (5.12) in terms of p_T and y: In terms of p_T and y, the phase space factor is constant in both variables, **no region is weighted more than any other**.

In the following, we explore two of the most representative processes that can take place in hadron-hadron collisions: the Drell-Yan process and inclusive jet production.

5.2 Drell-Yan production in hadronic collisions

Let us consider now the hadroproduction of massive vector bosons, namely the process

$$p + p \to V + X\,, \qquad V = W^+, W^-, Z\,, \tag{5.28}$$

where X denotes the rest of the produced hadronic final state, in addition to the vector boson, and the underlying partonic process is $q + \bar{q} \to \gamma^*/Z^0$ (neutral current) and $q + \bar{q}' \to W^\pm$ (for charged current production). Here we will work at the Born level only. Including radiative corrections would be possible following the techniques of the previous lectures. The corresponding Feynman diagram for the production and decay of a Z boson can be seen in Fig. 5.3. Using the Feynman rules for the production of a massive vector boson in electroweak theory (assuming for simplicity a generic value of the electroweak coupling g), one obtains

$$\mathcal{M} = g\, \hat{v}(p_2)\, \gamma^\mu\, u(p_1)\,, \tag{5.29}$$

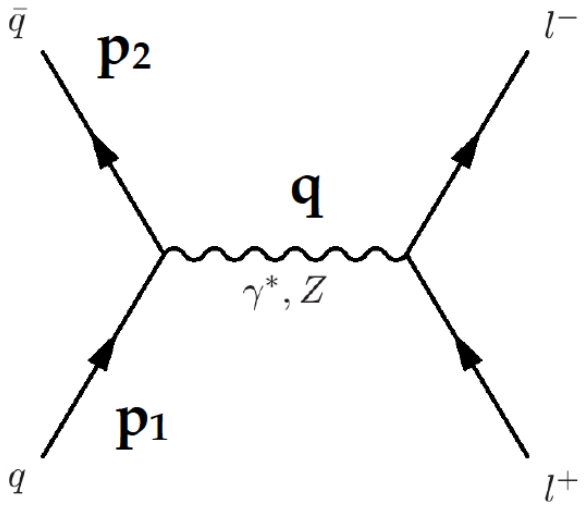

Figure 5.3. Feynman diagram for the hadroproduction of a neutral gauge boson, followed by the decay into two leptons, in the Born approximation. The four-momenta of the incoming quarks are labeled as p_1 and p_2.

where p_1 and p_2 label the four-momenta of the incoming quarks, and therefore the partonic cross-section reads, including the phase space factor,

$$\hat{\sigma} = \frac{1}{2\hat{s}} \frac{1}{4} \frac{1}{9} \int d\phi_1 \sum_{\text{spin,col}} |\mathcal{M}|^2 \tag{5.30}$$

where we have added the flux factor $1/2\hat{s}$, the average over initial state polarizations $1/4$ and the average over initial state colors $1/N_c^2$. Using the properties of the Dirac algebra, we find that the spin averaged matrix element squared is

$$\sum_{\text{spin,col}} |\mathcal{M}|^2 \, = \, 3g^2 \text{Tr} \left[\not{p}_1 \, \gamma^\mu \, (-\not{p}_2) \, \gamma_\mu \right] = 12 \, g^2 \, \hat{s} \, , \tag{5.31}$$

where we have used that

$$\text{Tr} \left[\not{p}_1 \, \gamma^\mu \, (-\not{p}_2) \, \gamma_\mu \right] = 8 p_1 \cdot p_2 \simeq 4 \, (p_1 + p_2)^2 = 4 \hat{s} \, , \tag{5.32}$$

neglecting the masses of the incoming quarks. Doing the calculation, we find that that total partonic cross-section is

$$\hat{\sigma} = \frac{4\pi^2}{3} \frac{g^2}{4\pi} \, \delta(\hat{s} - M_V^2) \tag{5.33}$$

where we have used that the one-particle Lorentz-Invariant Phase Space factor reduces to the energy conservation delta function:

$$d\phi_1 \, = \, \int \frac{d^3 q}{2q^0 (2\pi)^3} (2\pi)^4 \delta^{(4)} (p_1 + p_2 - q) \, = \, 2\pi \, \delta((p_1 + p_2)^2 - M_V^2) \, , \tag{5.34}$$

as expected in the case of a $2 \to 1$ process where the phase space is trivial. From Eq. (5.33) we find that the Drell-Yan production cross-section at the Born level will only be different from zero when the partonic center of mass energy satisfies $\sqrt{\hat{s}} = m_V$. Since we have derived above the relation between partonic and hadronic center of mass energies, Eq. (5.6) we see that to produce a vector boson we need that the **momentum fraction of the colliding quarks** satisfy $x_1 x_2 s = M_V^2$, with s being the hadronic total energy. Only if x_1

and x_2 satisfy this condition, it is kinematically possible to produce a vector boson in pp collisions, at least at the Born level.

Discussion #5.3

In addition to energy conservation, the production of Z^0 or $W^{\pm}$ gauge boson in proton-proton collisions needs also to take into account the **flavors of the colliding quarks**. Let us discuss the following points:

(a) In the case of neutral current production, $pp \to Z^0$, indicate a few possible quark initial states that will contribute to the process. Which channels are expected to be dominant? Can we have partonic subprocesses such as $u\bar{c}$?

(b) Repeat in the case of charged current scattering, with either W^+ or W^- production. Can we have here have initial states of different generations, such as $u + \bar{b} \to W^+$?

The cross-section derived in Eq. (5.33) corresponds to the partonic interaction. To obtain the hadronic cross-section relevant for proton-proton collisions, we need to apply the prescription of the **QCD parton model**, namely:

- Multiply the partonic cross-section by the parton distribution functions $f_i(x)$ associated to the underlying partonic processes: in this case $q + \bar{q}$ for Z production and $q + \bar{q}'$ for $W^{\pm}$ production.
- Integrate over all allowed values of the momentum fractions x_1, x_2.
- If required, integrate over all the kinematic variables in the final state which are not considered for the measurement.

For the specific case of W^+ production, in the QCD parton model, and keeping only the contribution from the first generation of quarks and anti-quarks for simplicity, assuming a diagonal CKM mixing matrix, we obtain that the hadronic cross-section is given by the usual convolution over the PDFs:

$$\sigma_{W^+} = \int_0^1 dx_1 \int_0^1 dx_2 \left[f_u(x_1) f_{\bar{d}}(x_2) + f_{\bar{d}}(x_1) f_u(x_2) \right] \times \frac{\pi^2}{3} \frac{\alpha_{\rm QED}}{\sin^2 \theta_W} \delta(s x_1 x_2 - M_W^2) \,, \tag{5.35}$$

where $\sin^2 \theta_W = (1 - m_W^2/m_Z^2)$ is Weinberg's mixing angle. In Eq. (5.35) we account for the two different ways in which a $u\bar{d}$ pair can be found in the two colliding protons. Indeed, we select the scattering $u\bar{d}$ and $\bar{d}u$, where the first quark corresponds to the first proton, and likewise for the rest.

Discussion #5.4

Eq. (5.35) corresponds to the **inclusive cross-section**, which consider all possible values of the final state kinematics. Discuss why such a total inclusive cross-section is not a realistic observable that can be directly measured say by the LHC detectors. Which other experimental observables could instead be more interesting? And which is the **smallest value of the momentum fraction** x for which we need to know the PDFs before we can evaluate this inclusive cross-section?

Given that measuring a fully inclusive cross-section is not possible with realistic detectors, it makes sense to try to make theoretical predictions for **differential distributions**. With this motivation, let us take a closer look at the kinematics of this process. As we have shown above, the kinematics of vector-boson

production in hadronic collisions can be written as follows:

$$p_1 = (x_1 E_p, 0, 0, x_1 E_p) \tag{5.36}$$
$$p_2 = (x_2 E_p, 0, 0, -x_2 E_p) \tag{5.37}$$
$$q = ((x_1 + x_2) E_p, 0, 0, (x_1 - x_2) E_p) \tag{5.38}$$

with p_i being the partonic momenta, q the four-momentum of the gauge boson, and E_p is the energy of the proton beam. In this process, the kinematics are fixed once the gauge boson rapidity is specified. To verify this, we can use the definition of the vector-boson rapidity y_V to find:

$$y_V = \frac{1}{2} \log \frac{q_0 + q_z}{q_0 - q_z} = \frac{1}{2} \log \frac{x_1}{x_2} , \tag{5.39}$$

while as we know energy conservation requires:

$$x_1 \, x_2 \, s = M_W^2 , \tag{5.40}$$

which is of course consistent with the mass shell condition $q^2 = M_W^2$. Given that E_p is fixed and known, and the same for m_W, it follows that specifying y_V determines the values of x_1 and x_2 and hence fully specifies the kinematics of the Drell-Yan process (given that there is no other variable left unconstrained). Solving these equations, we see how indeed the values of the PDF Bjorken-x probed in this process are fixed once the vector-boson rapidity is specified:

$$x_1 = \frac{M_W}{\sqrt{s}} e^{y_V} , \qquad x_2 = \frac{M_W}{\sqrt{s}} e^{-y_V} , \tag{5.41}$$

where note that y_V can be either positive or negative. Therefore, measuring the cross-section of vector boson production as a function of the rapidity y_V provides **direct information on the distribution of momentum fractions** x for the relevant quarks and antiquarks within the proton.

Rapidity coverage of vector-boson production

The relations derived in Eq. (5.41) enable us to determine the coverage in (x_1, x_2) that a given collider has access to. For instance, at the LHC with $\sqrt{s} = 14$ TeV, the ATLAS and CMS have a pseudo-rapidity coverage of $\eta \lesssim 2.5$. Assuming a vector boson produced with $y_V = 2.5$, we find that the underlying partonic kinematics will be x_1 (x_2) = 0.07 (0.0005), while for the LHCb detector, whose acceptance goes up to $y \leq 4.5$, a vector boson produced with $y_V = 4.5$ would correspond to x_1 (x_2) = 0.5 ($6\,10^{-5}$). Therefore, the measurements at forward rapidity cover a wider range of Bjorken-x, which has both positive and negative consequences. Note also that there is a **maximum value for the rapidity** y_V which is kinematically allowed. Indeed, since $x_1 \leq 1$, we have that $y_V^{(\max)} = \ln \sqrt{s}/M_W \sim 5.2$. For higher values of the rapidity, the cross-section vanishes. Hence a detector which could access vector boson rapidities of up to $y_V \sim 5.2$ would in principle be able to measure the total inclusive cross-section in Eq. (5.35).

Carrying out the delta function integral in Eq. (5.35), we end up with the following result for the total

inclusive cross-section

$$\begin{aligned}\sigma_{W^+} &= \int dx_1\, dx_2\, \left[f_u(x_1) f_{\bar{d}}(x_2) + f_{\bar{d}}(x_1) f_u(x_2) \right] \times \frac{\pi^2}{3} \frac{\alpha_{\rm QED}}{\sin^2\theta_W} \delta(s x_1 x_2 - M_W^2) \\ &= \frac{\pi^2}{3} \frac{\alpha_{\rm QED}}{\sin^2\theta_W} \frac{1}{s} \int_0^1 \frac{dx_1}{x_1} \left[f_u(x_1) f_{\bar{d}}\left(\frac{M_W^2}{x_1 s}\right) + f_{\bar{d}}(x_1) f_u\left(\frac{M_W^2}{x_1 s}\right) \right] . \end{aligned} \tag{5.42}$$

To evaluate the differential distribution in terms of the W boson rapidity y_V, we can use the following relation related to Eq. (5.41),

$$dx_1 = \frac{M_W}{\sqrt{s}} e^{y_V} dy_V = x_1 dy_V \tag{5.43}$$

and therefore we obtain our first differential cross-section for an hadron collider process:

$$\frac{d\,\sigma_{W^+}}{d\,y_V} = \frac{\pi^2}{3} \frac{\alpha_{\rm QED}}{\sin^2\theta_W\, s} \left[f_u(x_1) f_{\bar{d}}\,(x_2) + f_{\bar{d}}(x_1) f_u\,(x_2) \right] \tag{5.44}$$

with x_1, x_2 determined via Eq. (5.41). This differential cross-section is determined entirely for the shape of the PDFs at the values of $x_{1,2}$ fixed by the kinematics, Eq. (5.41). Eq. (5.44) shows how a measurement of this distribution would enable direct constraints on the proton PDF.

Discussion #5.5

The derivation so far assumes that we can directly measure the production of $W^\pm, Z$ bosons in our detector. However this is not possible since massive vector bosons are **short-lived particles** and decay very quickly. Taking this into account, discuss:

- Which are possible final states for Z production? If I measure the decay products, can I reconstruct the value of the Z boson kinematics?
- Which are possible final states for W^+ production? In its decay mode to leptons, can I directly reconstruct the W boson kinematics? If this is not the case, which alternative observables can one measure?
- Does QCD play a role in describing these decays of vector bosons?

This derivation represents an oversimplification of the complete Drell-Yan process, to begin with because the have considered only $u\bar{d}$ scattering. In Fig. 5.4 we display the contribution of different partonic initial states to the rapidity distribution of W^+ bosons at the LHC 7 TeV. Is clear that the effects of the second generation are important and cannot be neglected.

Applications of the Drell-Yan process

Improving the theoretical accuracy in the theoretical prediction of the W boson kinematic distribution is important to extract fundamental parameters of the SM, like the W mass, that might provide indirect constraints on New Physics beyond the SM. A permille precision in a number of distributions is required to be able to perform a competitive measurement. See Fig. 5.5 for the results of the impact of the direct W mass measurement in the global electroweak fit.

Another simplication in our derivation so far is that Eq. (5.44) includes only the Born term. Using similar techniques as in the case of e^+e^- and DIS it can be shown that soft and collinear final state divergences are canceled between real and virtual diagrams in inclusive enough distributions, and that the initial state

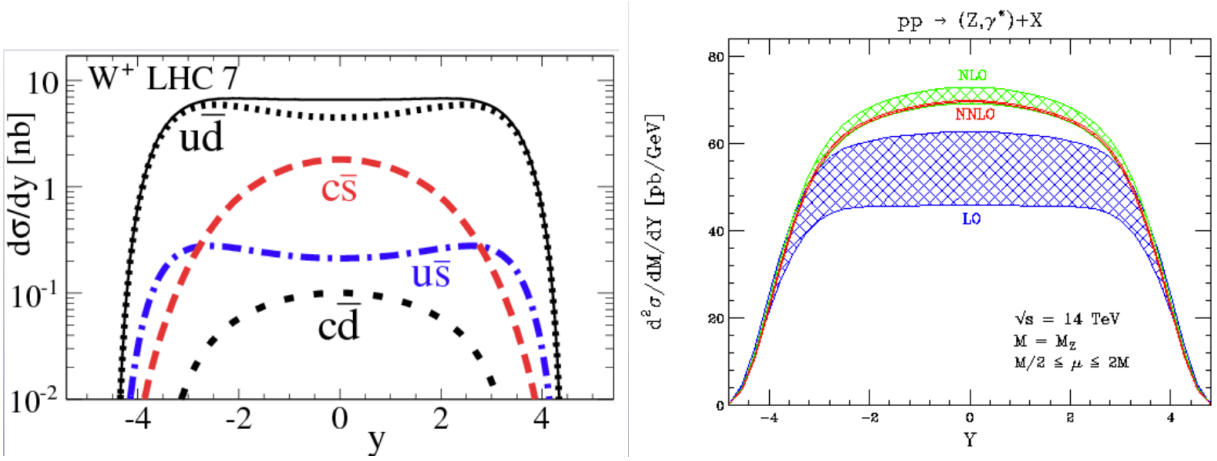

Figure 5.4. Left plot: the contribution of different partonic initial states to the rapidity distribution of W^+ bosons at the LHC 7 TeV. Right plot: the calculation of the rapidity distribution of Z bosons at the LHC 14 TeV, computed at LO, NLO and NNLO accuracy. The bands represent the theoretical uncertainty in the calculation arising from higher orders.

collinear singularity subtraction can be performed exactly in the same way as in the case of DIS. In the right plot of Fig. 5.4 we also show the calculation of the rapidity distribution of Z bosons at the LHC 14 TeV, computed at LO, NLO and NNLO accuracy. The bands represent the theoretical uncertainty in the calculation arising from higher orders, estimated by varying the renormalization and factorization scales with respect to the central scale.

Theory errors in QCD calculations

In hadron collider calculations, scale variations of the type $0.5 \leq \mu/\mu_F \leq 2$ and $0.5 \leq \mu/\mu_R \leq 2$ are used to estimate higher-order uncertainties. The basic idea is that since in the full calculation (resuming all orders) there is no dependence on this scales, we can estimate missing higher orders with a suitable scale variation. This procedure is know to work reasonable well for a number of cases, but not everywhere. In general, it remains an open question to find a fully reliable method to estimate missing higher orders in QCD perturbative calculations.

5.3 Jet production in proton-proton collisions

Another central process of hadron collider phenomenology is the production of jets. We have already encountered jets in our discussion of the $e^+ + e^- \to$ hadrons process, where we found that jets can be defined by means of a suitable **algorithmic procedure** which can be applied in the same way to parton-level, hadron-level, and detector-level calculations and simulations. Jets can be defined using a similar procedure in hadron-hadron collisions, and are actually the most frequent of all hard-scattering processes taking place at the LHC.

Jet production in pp collisions is the simplest hadroproduction $2 \to 2$ process with two colored parton in the initial state and two in the final state. To construct the jet cross-section at the Born level, we need to convolute all possible partonic cross-sections for the scattering of quarks and gluons with the corresponding parton distributions, in the same manner as we have done for vector-boson production in the Drell-Yan

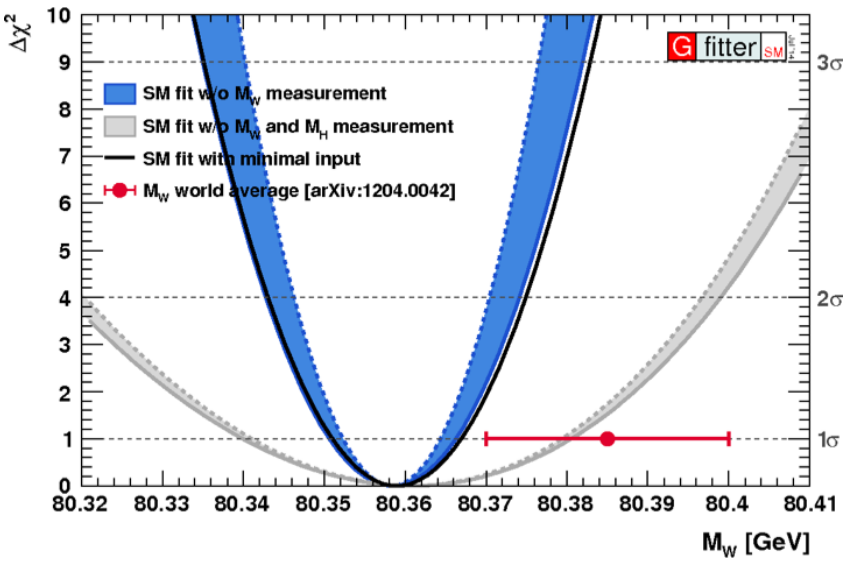

Figure 5.5. The impact of the direct W mass measurement in the global electroweak fit.

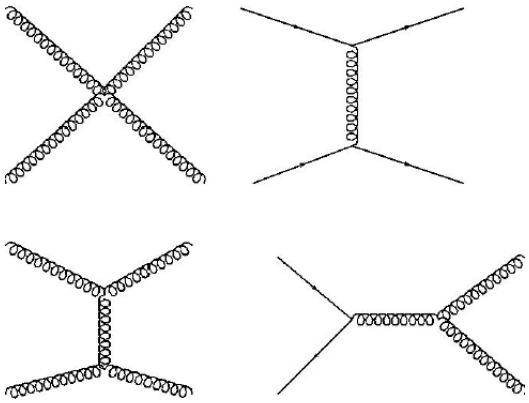

Process	$\frac{d\hat{\sigma}}{d\hat{\Phi}_2}$
$qq' \to qq'$	$\frac{1}{2\hat{s}}\frac{4}{9}\frac{\hat{s}^2+\hat{u}^2}{\hat{t}^2}$
$qq \to qq$	$\frac{1}{2}\frac{1}{2\hat{s}}\left[\frac{4}{9}\left(\frac{\hat{s}^2+\hat{u}^2}{\hat{t}^2}+\frac{\hat{s}^2+\hat{t}^2}{\hat{u}^2}\right)-\frac{8}{27}\frac{\hat{s}^2}{\hat{u}\hat{t}}\right]$
$q\bar{q} \to q'\bar{q}'$	$\frac{1}{2\hat{s}}\frac{4}{9}\frac{\hat{t}^2+\hat{u}^2}{\hat{s}^2}$
$q\bar{q} \to q\bar{q}$	$\frac{1}{2\hat{s}}\left[\frac{4}{9}\left(\frac{\hat{s}^2+\hat{u}^2}{\hat{t}^2}+\frac{\hat{t}^2+\hat{u}^2}{\hat{s}^2}\right)-\frac{8}{27}\frac{\hat{u}^2}{\hat{s}\hat{t}}\right]$
$q\bar{q} \to gg$	$\frac{1}{2}\frac{1}{2\hat{s}}\left[\frac{32}{27}\frac{\hat{t}^2+\hat{u}^2}{\hat{t}\hat{u}}-\frac{8}{3}\frac{\hat{t}^2+\hat{u}^2}{\hat{s}^2}\right]$
$gg \to q\bar{q}$	$\frac{1}{2\hat{s}}\left[\frac{1}{6}\frac{\hat{t}^2+\hat{u}^2}{\hat{t}\hat{u}}-\frac{3}{8}\frac{\hat{t}^2+\hat{u}^2}{\hat{s}^2}\right]$
$gq \to gq$	$\frac{1}{2\hat{s}}\left[-\frac{4}{9}\frac{\hat{s}^2+\hat{u}^2}{\hat{s}\hat{u}}+\frac{\hat{u}^2+\hat{s}^2}{\hat{t}^2}\right]$
$gg \to gg$	$\frac{1}{2}\frac{1}{2\hat{s}}\frac{9}{2}\left(3-\frac{\hat{t}\hat{u}}{\hat{s}^2}-\frac{\hat{s}\hat{u}}{\hat{t}^2}-\frac{\hat{s}\hat{t}}{\hat{u}^2}\right)$

Figure 5.6. Left plot: a representative subset of the Feynman diagrams that contribute to the hadroproduction jet cross-section at the Born level. Right plot: the result for the partonic cross-sections for different scattering channels.

process. The fully differential jet cross-section will be given by

$$d\sigma^{\rm jet} = \sum_{ijkl} dx_1\, dx_2\, f_i(x_1)\, f_j(x_2)\, \frac{d\hat{\sigma}_{ij\to kl}}{d\Phi_2}\, d\Phi_2\,, \tag{5.45}$$

where the partonic cross-section $d\hat{\sigma}_{ij\to kl}/d\Phi_2$ can be computed using the QCD Feynmann rules. In Fig. 5.6 we show some representative diagrams for the quark and gluon scattering processes that contribute to the jet cross-section. Note the presence of genuine QCD vertices like three and four gluon vertices. In Fig. 5.6 we also show the results for the calculation of all the various partonic cross-sections for different initial and final state combinations. The results are expressed in terms of $\hat{s}$, $\hat{t}$ and $\hat{u}$, the Mandelstam variables of the partonic scattering. While here we will work in the Born approximation, final and initial state soft singularities can be dealt as usual in pQCD, either absorbing them in PDF redefinitions or with a suitable jet algorithm.

Let us take a closer look at the kinematics of jet production, which are a bit different from the kinematics

of the Drell-Yan process since:

- The Drell-Yan process, $pp \to V$, is a $2 \to 1$ process. The initial state depends on two unknown variables, x_1 and x_2. Using momentum conservation $p_1 + p_2 \to q$ and the mass-shell condition $q^2 = M_W^2$, we find that a measurement of y_V fully specifies the process kinematics.
- Jet production is instead a $2 \to 2$ process, $p + p \to \text{jet} + \text{jet}$, since the final partonic state contains two partons. Hence we need more final-state variables to reconstruct the kinematics, also since now there is no mass-shell condition (p^2_{jet} is not constrained to take a specific value). Two final-state four-momenta without mass-shell constraints contain 8 unknowns. These are reduced to four using four-momentum conservation in terms of x_1 and x_2. So in principle we need to measure four independent final state variables to fully specify the kinematics.

For a $2 \to 2$ scattering of massless particles the kinematics are fully specified by the p_T of the back-to-back particles and by their rapidities y_1 and y_2. Therefore we can write the four-momentum of the two final-state quarks or gluons as

$$\begin{aligned} p_1 &= (p_T \cosh\, y_1, p_T \cos\phi, p_T \sin\phi, p_T \sinh\, y_1) \\ p_2 &= (p_T \cosh\, y_2, -p_T \cos\phi, -p_T \sin\phi, p_T \sinh\, y_2) \end{aligned} \tag{5.46}$$

where the rapidities $y_{1,2}$ are measured in the detector (laboratory) reference frame. Applying momentum conservation, we see that the values of the Bjorken-x that jet production is probing is given by

$$x_1 = \frac{p_T}{\sqrt{s}} \left(e^{y_1} + e^{y_2}\right) , \qquad x_2 = \frac{p_T}{\sqrt{s}} \left(e^{-y_1} + e^{-y_2}\right) . \tag{5.47}$$

Therefore, to reconstruct the kinematics of the underlying partonic collision one needs to measure the kinematics of the two jets.

It is possible to show, using the above kinematics, that for a given $\sqrt{s}$ and pseudo-rapidity η, the kinematically maximum available p_T is

$$p_T^{\max} \simeq \sqrt{s} e^{-y}/2 \,. \tag{5.48}$$

Assume that parton masses can be neglected here, so we have that $y = \eta$. The $\eta = 0$ case is trivial: all the energy of the proton-proton collision goes into the p_T of the final state particles, and hence $p_T^{(\max)} \sim \sqrt{s}/2$. Note that such very high values of the transverse momenta will be heavily suppressed by the fall-off of PDFs at large-x.

The calculation of the matrix elements is simplified in the **partonic center of mass frame**, defined by the following condition for a $2 \to 2$ scattering:

$$y_1^* = -y_2^* \quad \to \quad y_1^* = \frac{1}{2}\left(y_1 - y_2\right) = -y_2^* \tag{5.49}$$

and we can show that the scattering angle with respect to the beam axis θ^* is determined by the difference of rapidities of the two jets

$$\cos\,\theta^* = \tanh y_1^* = \tanh\left(\frac{y_1 - y_2}{2}\right) . \tag{5.50}$$

What is the boost required in this transformation? From

$$y \quad \to \quad y' = y + \frac{1}{2} \log \frac{1-\beta}{1+\beta} \,, \tag{5.51}$$

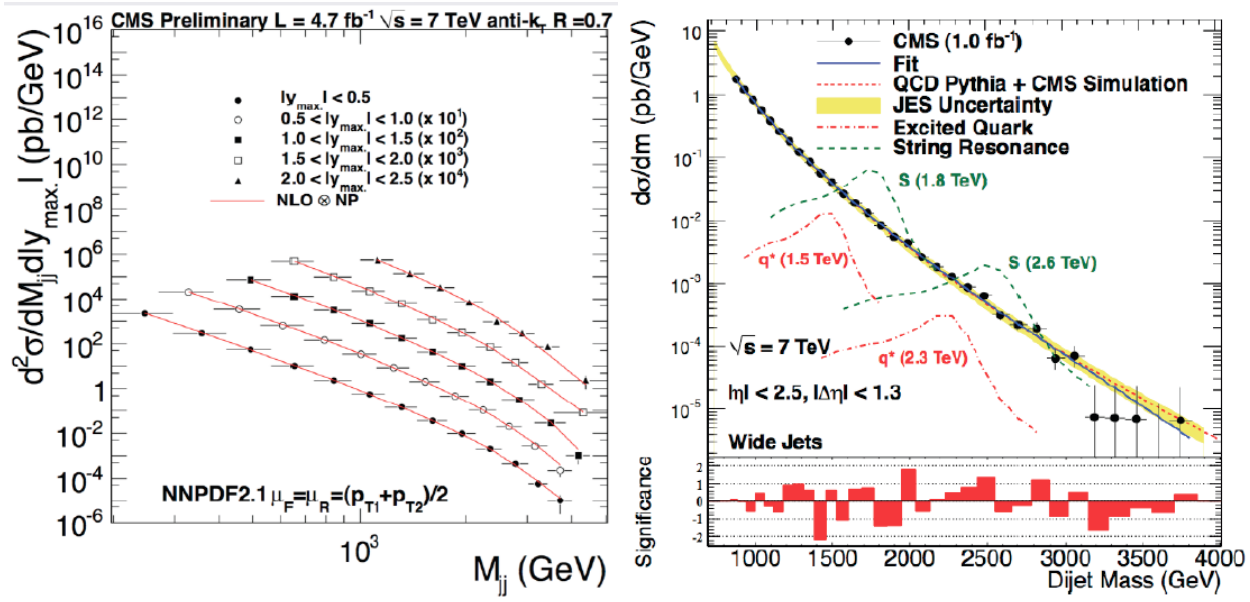

Figure 5.7. Left plot: the CMS measurement of the dijet cross-section at 7 TeV, compared with NLO QCD predictions with the NNPDF2.1 set. Right plot: the same observable, now used to search for New Physics that would appear as bumps in the otherwise smooth distribution due to new exotic particles being produced.

we see that

$$\frac{1}{2}\log\frac{1-\beta}{1+\beta} = -\frac{1}{2}(y_1+y_2)\,, \tag{5.52}$$

so the boost is determined by the PDFs in this particular event.

Another important kinematic variable is the invariant mass of the dijet system

$$M_{12}^2 = (p_1+p_2)^2 = 4\,p_T^2\,\cosh^2\,y^*\,, \quad M_{12} = 2\,p_T\,\cosh\,y^*\,. \tag{5.53}$$

which grows with the p_T of the jets and with their separation in rapidity (which is the same in the center-of-mass and laboratory reference frames). The fact that in dijet production we have a number of possible scales poses an important problem in our perturbative QCD calculations:

At hadron colliders, inclusive and dijet production are crucial properties to look for New Physics, as well as for the determination of fundamental strong coupling parameters such as $\alpha_S(M_Z)$ and the gluon PDF. In the case of QCD measurements, such as the M_{jj} invariant mass spectrum of dijets measured from CMS at 7 TeV, shown in Fig. 5.7, the comparison of the data with different PDFs provides direct information on the behavior of the gluon at large-x. The very same process can also be used for searches for BSM physics, for example, in Fig. 5.7 we show the dijet mass spectrum compared with the predictions for exotic scenarios like excited quarks or string resonances, that would show up as bumps in the otherwise smoothly falling distribution with M_{jj}. The absence of any noticeable bump allows them to place stringent limits in these scenarios for New Physics.

In the early 20-th century, the Rutherford experiment found evidence for the point like structure of the nuclei in atoms from the scattering of energetic α particles off a gold foil. In the 70s, the same idea was used in the SLAC deep-inelastic scattering experiments to find evidence of point-like constituents within the protons, the quarks, as we showed in Fig. 1.2. It is thus reasonable to expect that maybe quarks could in turn exhibit another layer of complexity, that could be identified in the same way, by scattering energetic particles, in this case other quarks and gluons, against quarks, at hadron colliders such as the LHC.

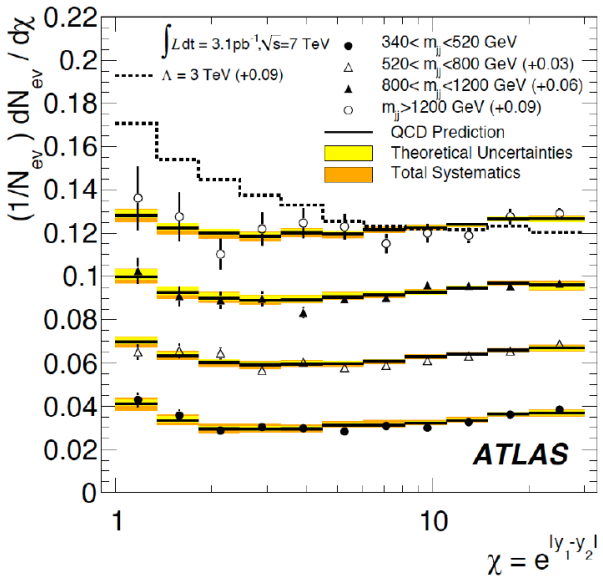

Figure 5.8. Measurement of the jet cross-section as a function of χ, where the QCD predictions are compared to a model with quark substructure, characterized by a scale $\Lambda = 3$ TeV.

To search for quark compositeness, the relevant scattering diagrams are those in the t-channel, for which the differential cross-section can be written as

$$\frac{d^2\sigma^{\rm jet}}{d\,M_{12}d\,\cos\theta^*} = \sum_{ij}\int_0^1 dx_1 dx_2 f_i(x_1) f_j(x_2)\delta(x_1 x_2\, s - M_{12})\frac{d\hat{\sigma}}{d\cos\theta^*} \tag{5.54}$$

where the partonic cross-section is (in the center of mass frame) nothing but the Rutherford cross-section for the scattering of point like particles from a Coulomb-like potential

$$\frac{d\hat{\sigma}}{d\cos\theta^*} \sim \frac{1}{\sin^4(\theta^*/2)} \tag{5.55}$$

Defining the variable χ, to remove the Rutherford singularity, we find that if quarks are point like we should find a flat cross-section as a function of χ:

$$\chi \equiv \frac{1+\cos\theta^*}{1-\cos\theta^*} \qquad \frac{d\hat{\sigma}}{d\chi} \propto \text{constant} \tag{5.56}$$

where we have used that

$$d\chi = 2d\cos\theta^*/(1-\cos\theta^*)^2\,. \tag{5.57}$$

This naive picture is of course complicated by higher order QCD effects, but in any case it remains true that any structure in the measured χ would hit towards quark substructure. A recent ATLAS search in this channel can be seen in Fig. 5.8. The QCD predictions, for point-like quarks, are in good agreement with the data showing that if quarks have substructure, this should appear at energy scales larger than $\Lambda = 3$ TeV.

To summarize, we have studied the predictions of QCD at hadron colliders, where the QCD factorization theorem ensures that the same PDFs that we measure in DIS can be used to make predictions at the LHC. We have studies two of the simplest, yet at the same time richest, process at hadron colliders: Drell-Yan and jet production, crucial both for BSM searches and for precision SM measurements. However, with fixed-order perturbative calculations we can describe only final states of low multiplicity, while real events involve

hundreds or thousands of particles. Moreover, QCD calculations are done in terms of quarks and gluons, while real event are composed by hadrons. Providing a realistic simulation of the hadronic final state can be achieved by the so-called Monte Carlo parton shower event generators, which are discussed now.

Discussion #5.6

Building up from what we have learned from the Drell-Yan processes and jet production at hadron-hadron colliders, we can now consider other processes of high relevance for LHC phenomenology. For each of these processes, let us draw the relevant Feynman diagrams and identify the **dominant partonic subprocesses**.

- D-meson production, for example with a $|c\bar{d}\rangle$ wave function.
- Top quark pair production. For this processes, discuss only which are the possible decay models and final states that can be accessed.
- Z-boson+jet production.
- Z-boson production in association with a charm quark.
- Direct photon production. Discuss here different ways in which a photon can be produced in a proton-proton collision.
- Three-jet production: which are the dominant tree-level diagrams?

You can also try to classify these various processes in terms of sensitivity to the proton PDFs. For example, if you would like to constrain the gluon PDF $g(x)$, which of the processes listed above appear to be more convenient?